

## Relationship between Structure, Entropy, and Diffusivity in Water and Water-Like Liquids

Manish Agarwal,<sup>†</sup> Murari Singh,<sup>†,‡</sup> Ruchi Sharma,<sup>†</sup> Mohammad Parvez Alam,<sup>†</sup> and Charusita Chakravarty<sup>\*,†</sup>

Department of Chemistry, Indian Institute of Technology—Delhi, New Delhi 110016, India, and School of Physical Sciences, Jawaharlal Nehru University, New Delhi 110067, India

Received: March 4, 2010; Revised Manuscript Received: April 13, 2010

Anomalous behavior of the excess entropy ( $S_e$ ) and the associated scaling relationship with diffusivity are compared in liquids with very different underlying interactions but similar water-like anomalies: water (SPC/E and TIP3P models), tetrahedral ionic melts ( $\text{SiO}_2$  and  $\text{BeF}_2$ ), and a fluid with core-softened, two-scale ramp (2SRP) interactions. We demonstrate the presence of an excess entropy anomaly in the two water models. Using length and energy scales appropriate for onset of anomalous behavior, we show the density range of the excess entropy anomaly to be much narrower in water than in ionic melts or the 2SRP fluid. While the reduced diffusivities ( $D^*$ ) conform to the excess-entropy-scaling relation,  $D^* = A \exp(\alpha S_e)$  for all the systems (Rosenfeld, Y. *Phys. Rev. A* **1977**, 15, 2545), the exponential scaling parameter,  $\alpha$ , shows a small isochore dependence in the case of water. Replacing  $S_e$  by pair correlation-based approximants accentuates the isochore dependence of the diffusivity scaling. Isochores with similar diffusivity-scaling parameters are shown to have the temperature dependence of the corresponding entropic contribution. The relationship between diffusivity, excess entropy, and pair correlation approximants to the excess entropy are very similar in all the tetrahedral liquids.

## 1. Introduction

Water displays a number of thermodynamic and kinetic anomalies when compared to simple liquids.<sup>1–3</sup> The density anomaly, corresponding to a negative isobaric thermal expansion coefficient ( $\alpha_P$ ), is the best known of these unusual properties of water and is observed for state points lying within an approximately parabolic boundary defined by the locus of temperatures of maximum density (TMD) for which  $\alpha_P = 0$ . The density anomaly implies the presence of other thermodynamic anomalies, such as those associated with the isobaric heat capacity ( $C_P$ ) and the isothermal compressibility ( $\kappa_T$ ). The kinetic anomalies of water are associated with an increase in molecular mobility on isothermal compression, measured in terms of diffusivity, orientational relaxation times, or viscosity. A number of network-forming inorganic melts with local tetrahedral order have been shown to possess water-like anomalies, most notably,  $\text{AB}_2$  ionic melts such as  $\text{SiO}_2$  and  $\text{BeF}_2$  and the liquid phase of elements, such as silicon and tellurium.<sup>4–15</sup> More recently, water-like anomalies have been demonstrated in mesoscopic liquids with isotropic, core-softened effective interactions or anisotropic patchy interactions.<sup>16–18</sup> Despite a very diverse set of underlying interactions, liquids with water-like anomalies are found to have essentially conformal liquid-state “phase diagrams” with a nested structure of anomalous regimes of density, diffusivity, and structural order.

The similarity in the phase diagrams of water-like liquids reflects similar structure–entropy–diffusivity relationships that can be conveniently analyzed in terms of the excess entropy,  $S_e$ , defined as the difference between the total thermodynamic entropy ( $S$ ) and the corresponding ideal gas entropy ( $S_{\text{id}}$ ) at the

same temperature and density. A necessary condition for a fluid to show water-like thermodynamic and transport anomalies is the existence of an excess entropy anomaly, corresponding to a rise in excess entropy,  $S_e$ , on isothermal compression ( $(\partial S_e / \partial \rho)_T > 0$ ).<sup>9–11,19–25</sup> Liquids with water-like anomalies display distinct forms of local order or length scales in the low- and high-density regimes; competition between the two types of local order results in a rise in excess entropy at intermediate densities. Most liquids, including anomalous ones, obey semiquantitative excess-entropy-scaling relationships for transport properties of the form  $X^* = A \exp(\alpha S_e)$  where  $X^*$  are reduced transport coefficients, and  $A$  and  $\alpha$  are scaling parameters that are very similar for systems with conformal potentials.<sup>26–29</sup> Consequently, the existence of an excess entropy anomaly is reflected in mobility anomalies. To make a more precise connection between thermodynamic and mobility anomalies, it is necessary to understand the assumptions underlying the scaling rule. Rosenfeld scaling assumes that diffusion in liquids takes place through a combination of binary collisions and cage relaxation. The binary collision contribution is approximately factored out by using macroscopic reduction parameters based on elementary kinetic theory. For example, reduced diffusivities are defined as  $D^* = D(\rho^{1/3}/(mk_B T))^{1/2}$ .<sup>27</sup> The frequency of cage relaxations is assumed to be proportional to the number of accessible configurations,  $\exp(\alpha S_e)$ , since configuration space connectivity is high in the stable liquid phase. For the scaling relationship to be state-point independent, it is necessary that the exponential parameter  $\alpha$  controlling the number of accessible configurations is determined by the interaction potential and is otherwise state-point independent.

This paper develops a basis for quantitative comparison of structure–entropy–diffusivity relationships in liquids with very different underlying interactions but similar water-like anomalies. We focus on three different categories of liquids: (i) molecular fluids ( $\text{H}_2\text{O}$ ), (ii) tetrahedral ionic melts ( $\text{BeF}_2$  and

\* Corresponding author. Tel: (+)91-11-2659-1510. Fax: (+)91-11-2686-2122. E-mail: charus@chemistry.iitd.ernet.in.

<sup>†</sup> Indian Institute of Technology.

<sup>‡</sup> Jawaharlal Nehru University.

**TABLE 1: State Point Corresponding to the Maximum Temperature along the TMD Locus ( $\rho_m$ ,  $T_m$ ) for the Systems Studied<sup>a</sup>**

	SPC/E <sup>30</sup>	TIP3P <sup>31</sup>	BeF <sub>2</sub> <sup>33</sup>	SiO <sub>2</sub> <sup>34</sup>	2SRP <sup>16</sup>
$\rho_m$ (g cm <sup>-3</sup> )	1.01	0.98	1.8	2.3	1.5
$T_m$ (K)	251	195	2310	5000	0.0548

<sup>a</sup> Potential parameters are given in the references. Values for the 2SRP are in the reduced units defined in the simulations details.

SiO<sub>2</sub>), and (iii) a core-softened fluid with isotropic, pair-additive interactions. Comparison of these different systems should provide very useful physical insights into the relationship between structure, entropy, and transport properties of liquids, including complex fluids, and has not been previously attempted. It is evident that parametric variations of a single functional form for the interaction potential are insufficient to serve as a basis for comparison of anomalous behavior for the three different categories of liquids studied here. Instead, we focus on directly comparing the two crucial features of the excess entropy relevant for water-like liquids: first, the presence of an excess entropy anomaly and, second, exponential scaling of transport properties with excess entropy. Since the state point, ( $\rho_m$ ,  $T_m$ ), corresponding to the maximum temperature along the TMD locus is a unique point common to all liquids with a water-like density anomaly, we use this information to define a natural energy and length scale for onset of anomalous behavior in each system.

The specific interaction models used for the different categories of liquids require some introductory comments. Anomalous behavior and scaling of transport properties with the thermodynamic excess entropy has so far not been studied in the case of water. Since the different water models are known to display anomalous properties at very different temperatures, we use two different effective pair potentials for water, TIP3P and SPC/E. The SPC/E model is known to qualitatively reproduce all anomalous properties of water but typically at temperatures that are 30–40 K lower than the experimental value of 279 K.<sup>2,4,29,30</sup> The TIP3P model is widely used in biomolecular simulations, but the onset temperature for anomalous behavior is 170–180 K.<sup>19,31,32</sup> The transferable rigid-ion model (TRIM) potential was used for BeF<sub>2</sub><sup>33</sup> and the van Beest–Kramer–van Santen (BKS) potential was used for SiO<sub>2</sub>.<sup>34</sup> As an example of a core-softened fluid with waterlike anomalies, we consider the two-scale ramp potential (2SRP).<sup>16,17</sup> Thus we study five different simulation models for the three categories of liquids. Table 1 summarizes some of the relevant information about these simulation systems at ( $\rho_m$ ,  $T_m$ ). Section 2 provides the necessary simulation details. Results are presented in section 3 and conclusions are discussed in section 4.

## 2. Simulation Details

Potential energy models for all systems studied here are given in Table 1. Molecular dynamics simulations of ionic melts (BeF<sub>2</sub> and SiO<sub>2</sub>) and water models (TIP3P and SPC/E) were performed in the *NVT* ensemble using the Verlet algorithm as implemented in the DL\_POLY package.<sup>35</sup> A temperature range of 1500–3000 K is studied for BeF<sub>2</sub> and 4000–6000 K for SiO<sub>2</sub>. Details of simulations of the two ionic melts are given in ref 36. Simulations of TIP3P and SPC/E water used 256 molecules in a cubic simulation box with 1 fs time step and production run lengths of 4–8 ns. Rigid-body constraints were maintained using the SHAKE algorithm. The Berendsen thermostat time constant,  $\tau_B$ , is 1 ps for SPC/E for all state points except those along the

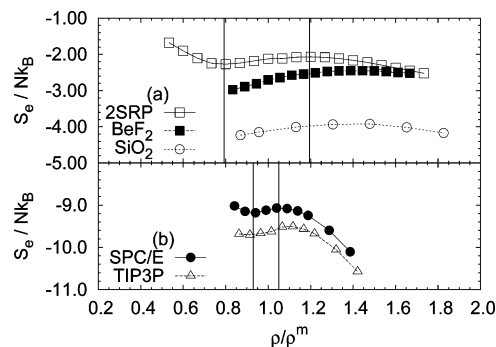


**Figure 1.** Plot of excess entropy  $S_e$  with scaled number density,  $\rho/\rho_m$ , for (a) ionic melts and 2SRP fluid and (b) water models. The lines mark the respective minima and maxima in the 2SRP fluid in (a) and the SPC/E model in (b).

210 K isotherm ( $\tau_B = 200$  ps) while  $\tau_B = 20$  ps for all TIP3P state points. State points for SPC/E water covered a temperature range from 210 to 300 K and a density range from 0.9 to 1.4 g cm<sup>-3</sup>; the temperature range for TIP3P water was kept as 170–300 K.

Simulations of the two-scale ramp potential (2SRP) fluid were performed using Metropolis Monte Carlo simulations using 256 particles in a cubic simulation box. The 2SRP fluid has length scales associated with the hard-core ( $\sigma_0$ ) and soft-core ( $\sigma_1$ ) diameters; we use  $\sigma_1$  as the unit of length. The energy  $U_1$  of the linear ramp interaction extrapolated to zero separation is taken as the unit of energy. State points cover a temperature range of 0.025 to 0.2 and density range from 0.8 to 2.6 in reduced units.<sup>9</sup> Diffusivities for five isotherms from  $T = 0.027$  to  $T = 0.063$  were taken from ref 37.

The Widom insertion method was used to calculate chemical potential and excess entropy for the 2-scale ramp fluid at low densities and high temperatures.<sup>38</sup> Thermodynamic integration was then used to obtain excess entropies at other state points. For ionic melts,  $S_{id}$  is computed for a noninteracting multicomponent mixture of atoms with the same masses and mole fractions as the ionic melt. Excess entropies for BeF<sub>2</sub> and SiO<sub>2</sub> melts were calculated using the same procedure as in ref 19, but over a more extensive density range. The excess entropy of the water models was computed relative to an ideal gas of rigid triatomic molecules at 1000 K, 0.01 g/cm<sup>3</sup>. Thermodynamic integration was used to compute  $S_e$  at other state points.<sup>4</sup> Our entropies at 298 K and 1 g cm<sup>-3</sup> match those of ref 39 for SPC/E and TIP3P, within statistical error. The use of atom–atom RDFs in eq 1 would suggest that an ideal gas reference state analogous to that used for ionic melts would be more appropriate; this is in fact not necessary, since the difference between the two reference states will be constant at a given temperature and density. We note that while the system sizes were chosen to be small enough that a large number of state points could be efficiently covered, they are sufficiently big that finite-size effects would be expected to make only small quantitative differences to the computed values of thermodynamic and transport properties.

## 3. Results

**3.1. Excess Entropy Anomaly.** The strength of the excess entropy anomaly determines the presence of diffusional, density, and related anomalies and reflects the variation in structural order in a fluid as a function of density. Figure 1 compares the density dependence of the excess entropy along the  $T = T_m$  isotherm, scaling densities with respect to the  $\rho_m$  value of each

system. While the overall behavior of  $S_e(\rho/\rho_m)$  is very similar, it is immediately apparent that, in units of  $\rho_m$ , the water models have a relatively narrow density regime of anomalous behavior and a steeper slope in the high density regime. The two-scale ramp (2SRP) system, in contrast, has a much wider anomalous regime bounded by a well-defined minimum as well as a maximum in  $S_e(\rho)$  along the  $T_m$  isotherm. The two ionic melts resemble the ramp fluid in the density range of anomalous behavior and the location of the maximum in  $S_e(\rho/\rho_m)$ . The minimum in the  $S_e(\rho/\rho_m)$  curves could not, however, be located within the density range, consistent with the thermodynamic stability criterion that the isothermal compressibility should be positive. In units of  $Nk_B$ , the rise in the  $S_e(\rho)$  curves from the minimum to the maximum is a fraction of a  $k_B$  for all the systems. This small anomaly is, however, sufficient to create an inflection point in the total  $S(\rho) = S_{id} + S_e$  curves that marks the onset of the density anomaly. The qualitative behavior of the excess entropy anomaly is consistent with the grouping of the fluids into three similar classes: rigid water models, ionic melts, and core-softened fluids. Unless otherwise stated, results for only one member of each class will be discussed in the rest of this paper.

**3.2. Excess Entropy Scaling of Diffusivities.** A comparison of the excess entropy scaling of the diffusivities for the different systems studied in this work, shown in Figure 2, illustrates that such a scaling approach is a reasonable predictor of diffusivities though there are small system-dependent differences. The 2SRP fluid shows excellent scaling for the state points studied, but the range of variation of the diffusivities is small in comparison to both ionic melts and water, given temperature variations by factors of 2–3. Both  $\text{SiO}_2$  and  $\text{BeF}_2$  show very good scaling in the liquid regime, but there is a change in slope  $\alpha$  for the lowest temperature isotherms, possibly due to the onset of cooperative dynamics.<sup>21,22,36,40,41</sup> The water models all show a distinct isochore dependence of the  $\ln D^*$  versus  $S_e$  plots, which is less pronounced in ionic melts and is essentially zero in the 2SRP fluid. In the case of water, deviations from linearity are specially noticeable at low temperatures for the 0.90 and 1.40 g cm<sup>-3</sup> isochores for which the mode-coupling temperature is relatively high.<sup>42</sup> All liquids with water-like anomalies are associated with a competition between two different length scales or local order metrics as a function of density. Therefore deviations from corresponding states behavior would be expected. It appears, however, that these deviations are small and most noticeable in the case of water, which has a rigid, nonspherical structure. Possible reasons for this are discussed below.

**3.3. Pair Correlation Estimators of the Excess Entropy.** The effect of the underlying structural correlations in a fluid on the entropy-transport relationships can be understood by expressing  $S_e$  as a multiparticle correlation expansion,  $S_e = S_2 + S_3 + \dots$ , where  $S_n$  is the entropy contribution due to  $n$ -particle spatial correlations.<sup>43–45</sup> The entropy contribution due to pair correlations between atoms of type  $\alpha$  and  $\beta$  is given by:

$$S_{\alpha\beta} = \int_0^\infty \{g_{\alpha\beta}(r) \ln g_{\alpha\beta}(r) - [g_{\alpha\beta}(r) - 1]\} r^2 dr \quad (1)$$

where  $g_{\alpha\beta}(r)$  is the atom–atom pair distribution function (PDF). The overall pair correlation entropy,  $S_2$ , is  $S_2/Nk_B = -2\pi\rho\sum_{\alpha,\beta}x_\alpha x_\beta S_{\alpha\beta}$ , where  $N$  is the number of particles and  $x_\alpha$  is the mole fraction of component  $\alpha$  in the mixture.  $S_2$  can be estimated from experimental scattering data as well as simulations and is the dominant contribution to the excess entropy in the case of simple<sup>44</sup> and core-softened fluids (e.g., results for

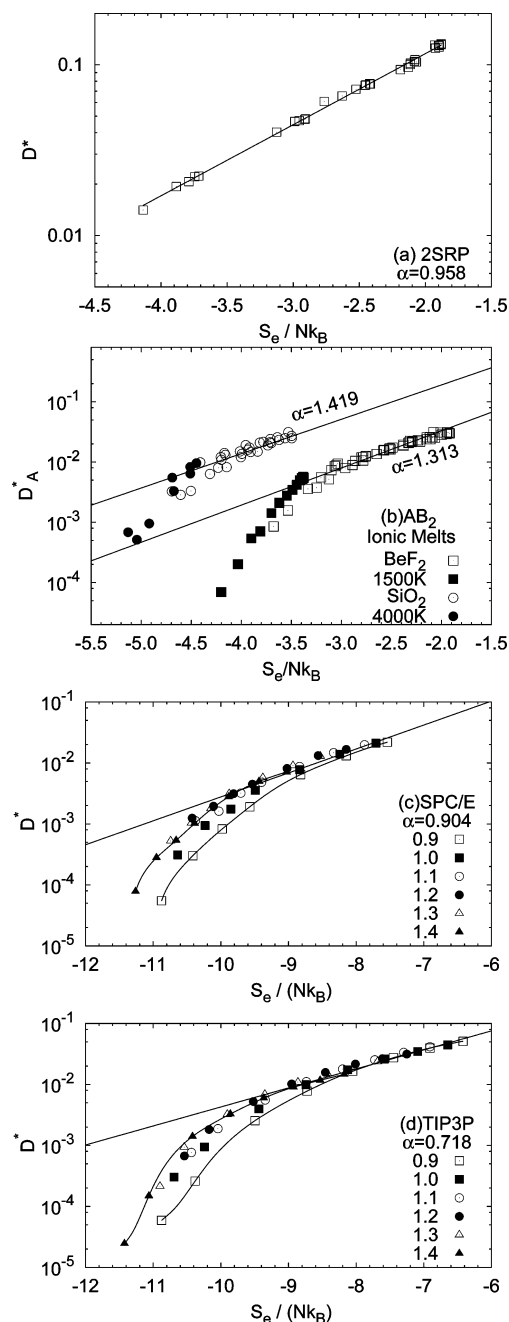


**Figure 2.** Correlation plots of Rosenfeld-scaled diffusivities with excess entropy,  $S_e$  of (a) two-scale ramp potential (2SRP) fluid, (b)  $\text{AB}_2$  ionic melts ( $\text{BeF}_2$  and  $\text{SiO}_2$ ), (c) SPC/E and (d) TIP3P. The lowest isotherms for  $\text{BeF}_2$  and  $\text{SiO}_2$  are shown with filled symbols. Data points lying along the highest and lowest isochore for (c) and (d) are joined with smooth lines. The scaling parameter  $\alpha$  for each plot is shown. In (b), the data points at 1500 K ( $\text{BeF}_2$ ) and 4000 K ( $\text{SiO}_2$ ) are shown as filled symbols and are excluded from the fit. In (c) and (d), data points having  $S_e < -9.5$  are excluded from the fit.

2SRP fluid in this paper), ionic melts, and water.<sup>19</sup> In the case of the  $\text{AB}_2$  melts and water, we also compute the tetrahedral correlation entropy,  $S_{AA}$ , due to the pair correlations between the tetrahedral (A) atoms, corresponding to Be, Si, and O in  $\text{BeF}_2$ ,  $\text{SiO}_2$ , and  $\text{H}_2\text{O}$ , respectively. The  $S_{OO}$  entropic contribution is reproduced by many coarse-grained model potentials of water that replace each water molecule by a structureless particle with isotropic effective interactions that reproduce the behavior of  $g_{OO}(r)$ .<sup>46,47</sup>

**3.3.1. Diffusivity Scaling.** The effect of using a structure-based approximant to the excess entropy, such as  $S_2$ , on the

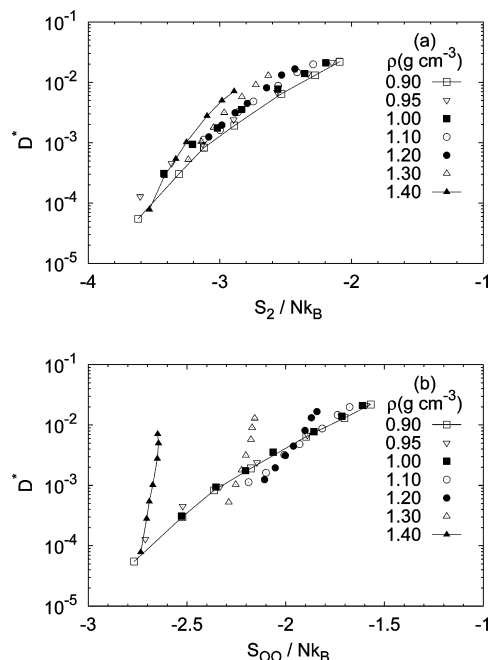


**Figure 3.** Correlation plots of Rosenfeld scaled diffusivities,  $D^*$ , in SPC/E water with (a)  $S_2$  and (b)  $S_{OO}$  for selected isochores. Straight lines connect data from the highest and lowest density isochores.

Rosenfeld-scaling relation can be seen by substituting  $S_e = S_2 + \Delta S$  to obtain

$$D^* \approx A \exp(\alpha S_e) = A \exp[\alpha S_2(1 + \Delta S/S_2)] = A \exp(\alpha' S_2) \quad (2)$$

where the new exponential scaling parameter,  $\alpha' = 1 + \Delta S/S_2$ , has a state-point dependence that is determined by the density and temperature-dependent behavior of  $\Delta S/S_2$ . Thus by using different approximants to the excess entropy and observing the effect on the scaling behavior of the transport properties, one can determine the importance of different structural correlations in controlling mobility. Figure 3 shows the correlation between the dimensionless diffusivity ( $D^*$ ) and  $S_2$  as well as  $x_{OO}^2 S_{OO}$  for SPC/E water, which should be compared with the results in Figure 2a. It is immediately obvious that the temperature dependence along an isochore is linear or quasi-linear, but there is a distinct isochore dependence of the slope  $\alpha$  of the  $\ln D^*$  versus  $S_\mu$  plots. The isochore dependence is most pronounced for  $S_\mu = S_{OO}$  and least pronounced for  $S_\mu = S_e$ . While the  $\ln D^*$  versus  $S_2$  or  $S_{AA}$  behavior has been studied before,<sup>12,23,25,36</sup> no systematic comparison with  $S_e$  and  $S_2$  scaling has been made so far. The ionic melts show a parallel behavior to the water models, in terms of diffusivity scaling with respect to  $S_e$ ,  $S_2$ , and  $S_{AA}$  while the 2SRP fluid also shows a small isochore dependence when  $D^*$  is scaled with respect to  $S_2$ . In the case of BeF<sub>2</sub>, the diffusivity and viscosity scaling with respect to  $S_e$  and  $S_2$  is given in refs 12 and 36 and with respect to  $S_{BeBe}$  in Supporting Information Figure 1. Scaling with respect to both  $S_e$  and  $S_2$  for the 2SRP fluid is shown in Supporting Information Figure 2. This is in contrast to simple liquids with pair additive potentials where excess-entropy-scaling relationships based on  $S_e$  and  $S_2$  have a similar degree of universality.<sup>28</sup>

**3.3.2. Temperature Dependence.** The isochore dependence of diffusivity scaling with different entropic contributions, and the contrast with simple liquids, suggest that the isochoric temperature dependence of different entropic measures deter-

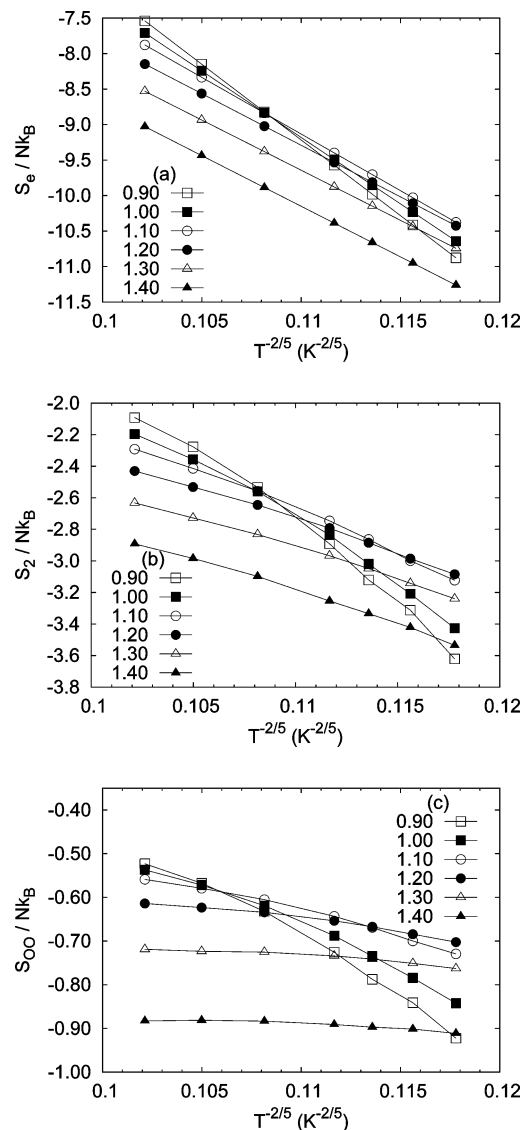


**Figure 4.** Different entropic contributions in SPC/E as a function of  $T^{-2/5}$ : (a) thermodynamic excess entropy,  $S_e$ ; (b) pair correlation entropy,  $S_2$ ; (c) entropic contribution due to oxygen–oxygen pair correlations,  $x_{OO}^2 S_{OO}$  with  $T^{-2/5}$ .

mines the quality of entropy–diffusivity scaling. On the basis of measure-free density functional theory for repulsive potentials, Rosenfeld predicted a  $T^{-2/5}$  scaling for the excess entropy.<sup>48</sup> In the case of simple liquids, these predictions are satisfied by both  $S_e$  and  $S_2$  and Rosenfeld scaling holds very well.<sup>48,49</sup>  $S_e$  is known to show  $T^{-2/5}$  scaling in ionic melts and water over the temperature regime of interest in this study.<sup>4,6</sup> Figure 4 shows  $S_e$ ,  $S_2$ , and  $S_{OO}$  as a function of  $T^{-2/5}$  for different isochores in SPC/E water. Unlike in simple liquids,  $S_2$  and  $S_{OO}$  show significant deviations from  $T^{-2/5}$  scaling in the anomalous regime. The results for BeF<sub>2</sub> are very similar to those of SPC/E water (see Supporting Information Figure 3 and refs 10 and 19). In the case of the 2SRP fluid, both  $S_e$  and  $S_2$  show deviations from  $T^{-2/5}$  behavior at low temperatures (see Supporting Information Figure 4).

A comparison of the isochore dependence of the Rosenfeld-scaling parameter with respect to an entropic contribution,  $S_\mu$ , and the temperature dependence of  $S_\mu$  shows that isochores with very different temperature dependences also have very different diffusivity-scaling parameters. For example, Figure 3b shows when  $\ln D^*$  is plotted as a function of  $S_{OO}$ , the slope increases



with increasing density and the three densest isochores, at  $\rho = 1.2, 1.3$ , and  $1.4 \text{ g cm}^{-3}$ , show very different and progressively increasing values of  $\alpha$ . Figure 4c shows that  $S_{OO}$  along these three isochores has a distinctly different and very weak temperature dependence. The two  $\text{AB}_2$  ionic melts show very similar patterns of behavior (see Supporting Information Figures 1 and 3), reflecting the similar structures of the tetrahedral fluids. The 2SRP fluid shows a weak isochore dependence of  $\alpha$  when  $S_e$  is replaced by  $S_2$ , which may be related to a spread of  $S_2$  values wider than those for  $S_e$ . It is interesting to note that  $S_2(T)$  and  $S_{AA}(T)$  curves show a much stronger density dependence than  $S_e(T)$ . In the case of the tetrahedral liquids, it is notable that at high densities,  $S_{AA}$  remains almost constant with temperature while diffusivity rises quite sharply. Since the overall excess entropy scaling for high and low density isotherms is not qualitatively different, this must imply that significant reorganization of the network associated with the other pair correlation contributions contributes to controlling diffusivity; for example, in water this could be strong librational-translational coupling reflected in the  $S_{OH}$  and  $S_{HH}$  contributions.

#### 4. Discussion and Conclusions

Excess entropy anomalies are compared in five liquids with water-like anomalies, with three completely different types of interactions: ionic melts ( $\text{BeF}_2$  and  $\text{SiO}_2$ ), hydrogen-bonded molecular liquid (SPC/E and TIP3P water), and core-softened fluid (two-scale ramp). Using the state point, ( $\rho_m$ ,  $T_m$ ), corresponding to the maximum temperature along the TMD locus to define energy and length scales, we show that excess entropy anomalies in the ionic melts and the core-softened fluid are very similar in range and strength, while the two water models have a conspicuously smaller density range and a much sharper decrease in  $S_e$  with density on strong compression.

We show that scaling of diffusivities with the thermodynamic excess entropy is good in all cases, noting that water is the first molecular fluid, other than the Lennard-Jones chain fluid,<sup>50</sup> for which Rosenfeld scaling with the thermodynamic excess entropy, rather than pair-correlation based estimators, has been tested. In comparison to ionic melts and the 2SRP fluid, a small isochoric dependence of the Rosenfeld-scaling parameters is seen in the case of water. This suggests the presence of additional length scales due to the rigid, nonspherical molecular shape, but these are not critical enough to destroy the overall correlation. The results for water suggest that Rosenfeld scaling will be useful for many other molecular fluids as a predictor of dynamical properties.

We examine the diffusivity scaling with two different entropy estimators based on pair correlation distribution functions (PDFs). The first one we refer to as the pair correlation entropy,  $S_2$ , includes information from all atom-atom PDFs. The second one, referred to as the tetrahedral correlation entropy ( $S_{AA}$ ), considers only the contribution from the pair correlations between the tetrahedral atom-atom PDFs and is applicable to only water and ionic melts. We show that the isochore dependence of the diffusivity-scaling parameters is most pronounced for  $S_{AA}$ , much less pronounced for  $S_2$ , and virtually negligible for  $S_e$ . Thus the state dependence of Rosenfeld-scaling parameters increases as the structural approximants to the entropy become poorer. We demonstrate that isochores with similar temperature dependences of the entropy estimators show very similar Rosenfeld-scaling parameters.

The clear correspondence between the isochoric Rosenfeld-scaling parameters and the temperature dependence of the entropy along isochores has an interesting implication. The

isochoric temperature dependence of the excess entropy of many atomic systems obeys a  $T^{-2/5}$  scaling, possibly because of the critical role of strong, short-range repulsions.<sup>48</sup>  $S_2$  shows a similar  $T^{-2/5}$  dependence in simple liquids but not in anomalous fluids, as shown in this study and elsewhere.<sup>11,19,49</sup> This suggests that diffusivities for many atomic fluids will obey Rosenfeld scaling best when the thermodynamic excess entropy is used. The 2SRP fluid presents an interesting case in that Rosenfeld scaling is applicable though there are deviations from  $T^{-2/5}$  scaling. It would be interesting to examine these ideas in the context of recent work on strongly correlating fluids.<sup>51,52</sup>

Our results on structure-entropy-diffusivity relationships are experimentally testable. Atom-atom PDFs, diffusivities, and calorimetric entropy are experimentally accessible as a function of temperature and density (or pressure). A comparison of diffusivity scaling with the thermodynamic entropy as well as the O-O pair correlation entropy between water and methanol should itself be very interesting, because they are both molecular, hydrogen-bonded liquids. Methanol, unlike water, does not show pronounced liquid-state anomalies, and we expect that this will show up in the diffusivity scaling with respect to the oxygen-oxygen pair correlation entropy but not with respect to the thermodynamic excess entropy. Since the atom-atom RDFs can be measured for essentially all molecular and polymeric fluids, our results suggest that excess entropy scaling should have substantial predictive value when combined with structural data, provided the complete set of atom-atom RDFs is used for estimating the entropy. However, coarse-graining procedures that rely on mapping a subset of atom-atom PDFs will not necessarily preserve the thermodynamic state-point dependence of transport properties, especially in anomalous fluids, as has been noted in recent studies of coarse-grained potentials for water.<sup>46,47</sup>

Our results suggest that Rosenfeld scaling is valid for a wide range of simple and anomalous liquids. The deviations are small if the complete thermodynamic excess entropy is used, possibly because of the dominance of strong, short-range repulsions. A microscopic understanding of Rosenfeld scaling is, however, necessary to understand the occurrence and magnitude of deviations in different systems. One possible route to developing such a microscopic approach is to use energy landscape approaches that have proved very useful in the context of supercooled liquids.<sup>53,54</sup> Efforts to apply energy landscape analysis to understand Rosenfeld scaling in simple and anomalous liquids have been relatively few.<sup>46,55,56</sup>

Water-like liquids are systems where an additional length scale comes into play as a function of density and therefore deviations from Rosenfeld scaling may be expected. As discussed in this paper, deviations are, in fact, small in this case. An analogous set of systems could be those where an additional length scale emerges as a function of temperature, as in inverse melting systems.<sup>57</sup> Some of the recent work on Rosenfeld scaling in systems with finite repulsions, such as the Hertizian sphere and the Gaussian core,<sup>58-61</sup> can be understood in terms of deviations from Rosenfeld-scaling behavior due to the change in the character of binary collisions as well as the possibility of additional length scales as a function of density.

To summarize, the anomalous behavior of the excess entropy ( $S_e$ ) and the associated scaling relationship with diffusivity are compared in five liquids with water-like thermodynamic and transport anomalies: SPC/E and TIP3P water models,  $\text{SiO}_2$  and  $\text{BeF}_2$  ionic melts, and the two-scale ramp (2SRP) fluid. When suitable length and energy scales are defined for the onset of anomalous behavior, the density range of the excess entropy

anomaly in water is shown to be much narrower in water than in ionic melts or the 2SRP fluid. While the Rosenfeld prediction of an exponential dependence of reduced diffusivity ( $D^*$ ) on the excess entropy ( $S_e$ ),  $D^* = A \exp(\alpha S_e)$  is found to be almost quantitatively valid for all the systems, the exponential scaling parameter,  $\alpha$ , is found to show a small isochore dependence in the case of water, presumably due to the rigid molecular structure. Unlike in the case of simple liquids, this isochore dependence of the excess entropy scaling of the diffusivities is accentuated by replacing  $S_e$  by the pair correlation entropy,  $S_2$ , for all the systems. In the case of the  $AB_2$  ionic melts and water, the effect is more pronounced if the diffusivity is scaled with respect to the pair correlation entropy associated with the tetrahedral atoms. More interestingly, variations in the isochoric temperature dependence of the entropic contribution ( $S_e$ ,  $S_2$ , and  $S_{AA}$ ) are found to be correlated with variations in the isochore diffusivity-scaling parameters, suggesting that the organization of the energy landscape changes significantly with density. The tetrahedral liquids (ionic melts and water) show very similar structure–entropy–diffusivity relations. Our results suggest that by systematically considering systems that represent different types and degrees of deviation from assumptions underlying Rosenfeld scaling, interesting physical insights into the relationship between structure, thermodynamics, and transport in liquids can be obtained.

**Acknowledgment.** This work was financially supported by the Department of Science and Technology, New Delhi. M.A. thanks the Indian Institute of Technology–Delhi for an award of a Senior Research Fellowship. M.S. thanks the University Grants Commission, New Delhi, for an award of a Junior Research Fellowship. We thank Divya Nayar for assistance with some of the computations.

**Supporting Information Available:** Plots of scaled diffusivities with entropic contributions and of isochoric temperature dependence of entropy data. This material is available free of charge via the Internet at <http://pubs.acs.org>.

## References and Notes

- Mishima, O.; Stanley, H. E. The relationship between liquid, supercooled and glassy water. *Nature* **1998**, *396*, 329–335.
- Debenedetti, P. G. Supercooled and glassy water. *J. Phys.-Cond. Mat.* **2003**, *15*, R1669–R1726.
- Errington, J. R.; Debenedetti, P. G. Relationship between structural order and the anomalies of liquid water. *Nature* **2001**, *409*, 318–321.
- Scala, A.; Starr, F. W.; Nave, E. L.; Sciortino, F.; Stanley, H. E. Configurational entropy and diffusivity of supercooled water. *Nature* **2000**, *406*, 166–169.
- Shell, M. S.; Debenedetti, P. G.; Panagiotopoulos, A. Z. Molecular structural order and anomalies in liquid silica. *Phys. Rev. E* **2002**, *66*, 011202.
- Poole, P. H.; Hemmati, M.; Angell, C. A. Comparison of thermodynamic properties of simulated liquid silica and water. *Phys. Rev. Lett.* **1997**, *79*, 2281–2284.
- Hemmati, M.; Moynihan, C. T.; Angell, C. A. Interpretation of the molten  $BeF_2$  viscosity anomaly in terms of a high temperature density maximum, and other waterlike features. *J. Chem. Phys.* **2001**, *115*, 6663–6671.
- Tanaka, H. Simple view of waterlike anomalies of atomic liquids with directional bonding. *Phys. Rev. B* **2002**, *66*, 064202.
- Sharma, R.; Chakraborty, S. N.; Chakravarty, C. Entropy, diffusivity, and structural order in liquids with waterlike anomalies. *J. Chem. Phys.* **2006**, *125*, 204501.
- Agarwal, M.; Sharma, R.; Chakravarty, C. Ionic melts with waterlike anomalies: Thermodynamic properties of liquid  $BeF_2$ . *J. Chem. Phys.* **2007**, *127*, 164502.
- Agarwal, M.; Chakravarty, C. Waterlike structural and excess entropy anomalies in liquid beryllium fluoride. *J. Phys. Chem. B* **2007**, *111*, 13294–13300.
- Agarwal, M.; Chakravarty, C. Relationship between structure, entropy, and mobility in network-forming ionic melts. *Phys. Rev. E* **2009**, *79*, 030202.
- Molinero, V.; Moore, E. B. Water modeled as an intermediate element between carbon and silicon. *J. Phys. Chem. B* **2009**, *113*, 4008–4016.
- Sastry, S.; Angell, C. A. Liquid-liquid phase transition in supercooled silicon. *Nature Mat.* **2003**, *2*, 739–743.
- Kanno, H.; Yokoyama, H.; Yoshimura, Y. A new interpretation of anomalous properties of water based on Stillinger's postulate. *J. Phys. Chem. B* **2001**, *105*, 2019–2026.
- Jagla, E. A. Low-temperature behavior of core-softened models: Water and silica behavior. *Phys. Rev. E* **2001**, *63*, 061509.
- Yan, Z.; Buldyrev, S. V.; Giovambattista, N.; Stanley, H. E. Structural order for one-scale and two-scale potentials. *Phys. Rev. Lett.* **2005**, *95*, 130604.
- Sciortino, F. Gel-forming patchy colloids and network glass formers: thermodynamic and dynamic analogies. *Eur. Phys. J. B* **2008**, *64*, 505–509.
- Sharma, R.; Agarwal, M.; Chakravarty, C. Estimating entropy of liquids from atom-atom radial distribution functions: Silica, beryllium fluoride and water. *Mol. Phys.* **2008**, *106*, 1925–1938.
- de Oliveira, A. B.; Franzese, G.; Netz, P. A.; Barbosa, M. C. Waterlike hierarchy of anomalies in a continuous spherical shouldered potential. *J. Chem. Phys.* **2008**, *128*, 064901.
- Mittal, J.; Errington, J. R.; Truskett, T. M. Relationship between thermodynamics and dynamics of supercooled liquids. *J. Chem. Phys.* **2006**, *125*, 076102.
- Mittal, J.; Errington, J. R.; Truskett, T. M. Erratum: Relationship between thermodynamics and dynamics of supercooled liquids [*J. Chem. Phys.* **2006**, *125*, 076102]. *J. Chem. Phys.* **2010**, *132*, 169904.
- Mittal, J.; Errington, J. R.; Truskett, T. M. Quantitative link between single-particle dynamics and static structure of supercooled liquids. *J. Phys. Chem. B* **2006**, *110*, 18147–18150.
- Errington, J. R.; Truskett, T. M.; Mittal, J. Excess-entropy-based anomalies for a waterlike fluid. *J. Chem. Phys.* **2006**, *125*, 244502.
- Yan, Z.; Buldyrev, S. V.; Stanley, H. E. Relation of water anomalies to the excess entropy. *Phys. Rev. E* **2008**, *78*, 051201.
- Rosenfeld, Y. Relation between transport coefficients and the internal energy of simple systems. *Phys. Rev. A* **1977**, *15*, 2545–2549.
- Rosenfeld, Y. A quasi-universal scaling law for atomic transport in simple fluids. *J. Phys. Condens. Mat.* **1999**, *11*, 5415.
- Dzugutov, M. A universal scaling law for atomic diffusion in condensed matter. *Nature (London)* **1996**, *381*, 137–139.
- Hoyt, J. J.; Asta, M.; Sadigh, B. Test of the universal scaling law for the diffusion coefficient in liquid metals. *Phys. Rev. Lett.* **2000**, *85*, 594–597.
- Berendsen, H. J. C.; Grigera, J. R.; Straatsma, T. P. The missing term in effective pair potentials. *J. Phys. Chem.* **1987**, *91*, 6269–6271.
- Jorgensen, W. L.; Chandrasekhar, J.; Madura, J. D.; Impey, R. W.; Klein, M. L. Comparison of simple potential functions for simulating liquid water. *J. Chem. Phys.* **1983**, *79*, 926–935.
- Vega, C.; Abascal, J. L. F. Relation between the melting temperature and the temperature of maximum density for the most common models of water. *J. Chem. Phys.* **2005**, *123*, 144504.
- Woodcock, L. V.; Angell, C. A.; Cheeseman, P. Molecular dynamics studies of vitreous state: Simple ionic systems and silica. *J. Chem. Phys.* **1976**, *65*, 1565–1577.
- van Beest, B. W. H.; Kramer, G. J.; van Santen, R. A. Force fields for silicas and aluminophosphates based on ab initio calculations. *Phys. Rev. Lett.* **1990**, *64*, 1955–1958.
- Smith, W.; Yong, C. W.; Rodger, P. M. DL\_POLY: Application to molecular simulation. *Mol. Simul.* **2002**, *28*, 385–471.
- Agarwal, M.; Ganguly, A.; Chakravarty, C. Transport properties of tetrahedral, network-forming ionic melts. *J. Phys. Chem. B* **2009**, *113*, 15284–113.
- Kumar, P.; Buldyrev, S. V.; Sciortino, F.; Zaccarelli, E.; Stanley, H. E. Static and dynamic anomalies in a repulsive spherical ramp liquid: Theory and simulation. *Phys. Rev. E* **2005**, *72*, 021501.
- Frenkel, D.; Smit, B. *Understanding Molecular Simulation: From Algorithms to Applications*; Academic Press: London, 2002.
- Henchman, R. H. Free energy of liquid water from a computer simulation via cell theory. *J. Chem. Phys.* **2007**, *126*, 064504.
- Dzugutov, M. Dynamical diagnostics of ergodicity breaking in supercooled liquids. *J. Phys. Condens. Mat.* **1999**, *11*, A253.
- Kaur, C.; Harbola, U.; Das, S. P. Nature of the entropy versus self-diffusivity plot for simple liquids. *J. Chem. Phys.* **2005**, *123*, 034501.
- Starr, F. W.; Sciortino, F.; Stanley, H. E. Dynamics of simulated water under pressure. *Phys. Rev. E* **1999**, *60*, 6757–6768.
- Green, H. S. *The Molecular Theory of Fluids*; North-Holland: Amsterdam, 1952.
- Baranyai, A.; Evans, D. J. Direct entropy calculation from computer simulation of liquids. *Phys. Rev. A* **1989**, *40*, 3817–3822.

- (45) Laird, B. B.; Haymet, A. D. J. Calculation of entropy from multiparticle correlation functions. *Phys. Rev. A* **1992**, *45*, 5680–5689.
- (46) Johnson, M. E.; Head-Gordon, T. Assessing thermodynamic relationships for waterlike liquids. *J. Chem. Phys.* **2009**, *130*, 214510.
- (47) Chaimovich, A.; Shell, M. S. Anomalous waterlike behavior in spherically-symmetric water models optimized with the relative entropy. *Phys. Chem. Chem. Phys.* **2009**, *11*, 1901–1915.
- (48) Rosenfeld, Y.; Tarazona, P. Density functional theory and the asymptotic high density expansion of the free energy of classical solids and fluids. *Mol. Phys.* **1998**, *95*, 141–150.
- (49) Chakraborty, S. N.; Chakravarty, C. Entropy, local order, and the freezing transition in morse liquids. *Phys. Rev. E* **2007**, *76*, 011201.
- (50) Goel, T.; Patra, C. N.; Mukherjee, T.; Chakravarty, C. Excess entropy scaling of transport properties of Lennard-Jones chains. *J. Chem. Phys.* **2008**, *129*, 164904.
- (51) Gnan, N.; Schrøder, T. B.; Pedersen, U. R.; Bailey, N. P.; Dyre, J. C. Pressure-energy correlations in liquids. IV. “Isomorphs” in liquid phase diagrams. *J. Chem. Phys.* **2009**, *131*, 234504.
- (52) Pedersen, U. R.; Bailey, N. P.; Schrøder, T. B.; Dyre, J. C. Strong Pressure-Energy Correlations in van der Waals Liquids. *Phys. Rev. Lett.* **2008**, *100*, 015701.
- (53) Debenedetti, P. G.; Stillinger, F. H. Supercooled liquids and the glass transition. *Nature* **2001**, *410*, 259–267.
- (54) Karmakar, S.; Dasgupta, C.; Sastry, S. Growing length and time scales in glass-forming liquids. *Proc. Natl. Acad. Sci.* **2009**, *106*, 3675–3679.
- (55) Chakraborty, S. N.; Chakravarty, C. Diffusivity, Excess Entropy and the Potential Energy Landscape of Monoatomic Liquids. *J. Chem. Phys.* **2006**, *124*, 014507.
- (56) de Oliveira, A. B.; Salcedo, E.; Chakravarty, C.; Barbosa, M. C. Entropy, diffusivity and the energy landscape of a water-like fluid. arXiv:1002.3781v1 [cond-mat.soft].
- (57) Feeney, M. R.; Debenedetti, P. G.; Stillinger, F. H. A statistical mechanical model for inverse melting. *J. Chem. Phys.* **2003**, *119*, 4582–4591.
- (58) Krekelberg, W. P.; Kumar, T.; Mittal, J.; Errington, J. R.; Truskett, T. M. Anomalous structure and dynamics of the gaussian-core fluid. *Phys. Rev. E* **2009**, *79*, 031203.
- (59) Pamies, J. C.; Cacciuto, A.; Frenkel, D. Phase diagram of Hertzian spheres. *J. Chem. Phys.* **2009**, *131*, 044514.
- (60) Fomin, Y. D.; Gribova, N. V.; Ryzhov, V. N. Breakdown of The Excess Entropy Scaling for the Systems with Thermodynamic Anomalies. arXiv:1001.0111v1 [cond-mat.soft].
- (61) Krekelberg, W. P.; Pond, M. J.; Goel, G.; Shen, V. K.; Errington, J. R.; Truskett, T. M. Generalized Rosenfeld scalings for tracer diffusivities in not-so-simple fluids: Mixtures and soft particles. *Phys. Rev. E* **2009**, *80*, 061205.

JP101956U